Intravitreal Silicon-Based Quantum Dots as Neuroprotective Factors in a Model of Retinal Photoreceptor Degeneration

Jeffrey L. Olson,[1] Raul Velez-Montoya,[1] Naresh Mandava,[1] and Conrad R. Stoldt[2]

PURPOSE. To study the intravitreal application of silicon quantum dots (QDs) and their capabilities to deliver electrical stimulation to the retinal cells and to assess the potential effect on retinal electrophysiology and anatomy.

METHODS. A Royal College of Surgeon rat model of retinal degeneration was used in this study. A total of 32 eyes were used, divided in four groups of 8 eyes each; the first group received the silicon-based QD, the second group received an inactive gold-based QD, the third group received a sham injection, and the fourth group was used as a control. An electroretinogram (ERG) was done at baseline and thereafter every week for 9 weeks. At the end of the follow-up, eyes were collected for further pathologic analysis and nuclei cell counts.

RESULTS. Eyes within the silicon-based QD group showed a definite but transient increase in the waves of the ERG, especially in the rod response compared with the sham and control groups ($P < 0.05$). The pathologic examination demonstrated a higher nuclei count in the QD group, consistent with a higher cell survival rate than that in the sham and control groups in which cells degenerated as expected.

CONCLUSIONS. Intravitreal injection of silicon-based QD seems to be safe and well tolerated, with no evident toxic reaction and demonstrates a beneficial effect by prolonging cell survival rate and improving ERG patterns in a well-established model of retinal degeneration. (ClinicalTrials.gov numbers NCT00407602, NCT01490827.) (*Invest Ophthalmol Vis Sci.* 2012;53:5713–5721) DOI:10.1167/iovs.12-9745

Blinding retinal diseases affect millions of patients, creating huge economic and social implications worldwide.[1,2] According to the World Health Organization in 2004 there was an estimated 161 million people with visual impairment, including 37 million with blindness, a number projected to reach 76 million by year 2020.[3–5]

Regarding the pediatric population, there are 1.4 million blind children around the world with an incidence ranging from 3:10,000 to 15:10,000.[6,7] Retinal disorders account for 33% of these cases in which retinopathy of prematurity represents the most prevalent pathology (≈17.4%) and retinal dystrophies, although rare, represent the major causes of incurable familial blindness. Retinitis pigmentosa is the most frequent cause of inherited visual impairment, with a worldwide prevalence of 1:4000.[6,8]

The leading causes of blindness and visual impairment in the world are age-related macular degeneration (AMD), diabetic retinopathy, cataract, and glaucoma, which tend to occur in older individuals. Despite the advances in Western medicine in diagnosing and treating these illnesses, irreversible visual loss still occurs in a significant proportion of cases.[1,9–12]

In 2004, the direct medical cost in the United States of AMD alone was estimated at $575 million, excluding nursing home cost, productivity losses, and home health care cost incurred by those with AMD.[11,13] It has been estimated that the total cost of global blindness is approximately one fourth to one sixth of the United Kingdom's gross national product.[14,15] Therefore, there is certainly a medical, social, and economic drive for preventing vision loss before it occurs.

Loss of vision secondary to retinal disorders has a common denominator: the degeneration of the neural cells of the eye (photoreceptors, interneurons, and retinal ganglion cells) and essential supporting cells, such as the retinal pigment epithelium (RPE).[9,16,17] Once damage has occurred, the visual impairment is irreversible and untreatable by current standard therapeutic approaches.[9] Significant effort has been directed toward developing novel treatments using neuroprotective and regenerative strategies, trying to prevent or delay significant neural degeneration.[9,18–20]

The use of chronic or pulsed electrical stimulation (ES), as a neuroprotective therapy in neural diseases, is well documented.[21–23] Spinal cord injury, Parkinson's disease, diabetic neuropathy, and hearing loss are among the most promising candidate diseases to benefit from this therapeutic modality.[22–25] In the retina, the effects of direct ES are not fully understood; however, multiple animal models and human studies have demonstrated that electrical current, regardless of the route of delivery, may prevent or delay cell death in all three retinal nuclear layers.[26–28] It is believed that ES may induce the production of growth and survival factors, slowing the natural photoreceptor degeneration.[29,30]

Quantum dots (QDs) are nanometer-sized tunable semiconductor crystals (1–12 nm) with a narrow and nearly Gaussian emission spectra that can be excited at a single wavelength and broad absorption patterns.[31–33] They were one of the first nanotechnologies to be integrated with the biological sciences.[31,32] Their unique emission characteristics make them powerful probes for fluorescence multiplexing, single-molecule tracking, fluorescence resonance energy transfer, high-throughput screening, flow cytometry, cell motility assays, and sentinel lymph node mapping.[32,33] Their unique constitution enables a photoactive property similar to that of a bulk semiconductor such that when exposed to electromagnetic energy in the form of visible light, they can convert light into

an electrical impulse (photovoltaic response).[33,34] Further, QDs can be engineered to be sensitive to energy of different wavelengths (ultraviolet to infrared), behaving more like small solar cells, producing energy in response to light.[34–36] Within the eye, QDs have been used to improve imaging of the vitreous and for cell labeling in animal models.[37,38] Although they are considered safe for in vivo use, their potential toxicity depends on factors derived from their inherent physicochemical properties and environmental conditions such as size, charge, concentration, outer coating bioactivity, and mechanical stability.[33,39]

The objective of this study was to assess the capability to deliver electrical stimulation to the retinal cells by silicon-based QDs and to study their potential effect on retinal electrophysiology and anatomy through the implantation of these photoactive nanoparticles into a well-defined model of retinal degeneration.

METHODS

The study was reviewed and approved by the University of Colorado Institutional Animal Care and Use Committee. All procedures were performed according to the statement for the use of animals in ophthalmic and visual research from the Association of Research of Vision and Ophthalmology (ARVO). The study was conducted at the University of Colorado facilities.

Royal College of Surgeon (RCS) rats were used in this study. The rats were originally obtained from Machelle Pardue (Atlanta VA Medical Center); a breeding colony was maintained as a homozygous breeding colony at the Center for Comparative Medicine at the University of Colorado Denver, Anschutz Medical Campus. This particular breed has a mutation on the MERTK gene, a member of the MER/AXL/TYRO3 receptor kinase family that encodes a transmembrane protein associated with disruption on the retinal pigment epithelium phagocytosis pathway and onset of autosomal recessive retinitis pigmentosa.[40–42] RCS rats are a well-defined model for retinal degeneration, in which the retina suffers a deterioration of its electrical activity from the third week of life onward, with no recordable activity by week 12.[40,43] All animals were housed on a 12-hour light/dark cycle with food and water without restriction. All procedures are done using rats 4 weeks of age, with a range of 2 days older or younger to minimize variability and ensure that all rats were at the same chronologic stage of degeneration.

A total of 32 eyes were used in this study. The eyes were further divided into four groups of 8 eyes each: a control group with no intervention, a sham surgery group that received intraocular saline injections, and two QD groups. The first QD group received an intraocular implant of pure silicon-based QD (Meliorum, Rochester, NY) and the second group received an intraocular implant of pure gold-based QD (SPI Mark, West Chester, PA). Both QDs are colloidal semiconductor nanocrystals, suspended in an aqueous medium, and composed of a pure core made of silicon or gold with no shell or conjugated proteins. The silicon QDs, as provided by the manufacturer, have a sodium dodecylbenzenesulfonate surfactant coating that is not covalently bound to the surface. The gold nanoparticles (as stated on the manufacturer's website: http://www.2spi.com/catalog/chem/gold-4.php) are surface stabilized with negative charge and do not have surfactants or biological surface modifiers. Nevertheless, it is very likely that neither of the nanoparticles has a coating that survives exposure to biological media after injection due to small changes in the solution ion content or pH. The silicon QD gets excited by a wavelength of light up to 750 nm (near infrared spectrum). The gold QD gets excited by a wavelength around 520 nm (below fluorescent light threshold), making the latter a form of inactive implant. The animal laboratory was lighted with fluorescent light and the average luminance during the 12-hour light cycle was ≈120 lux and colorimetry ranging from 520 to 660 nm at all times.

Prior to intraocular injection, all animals were anesthetized using ketamine (80 mg/kg) and xylazine (5–10 mg/kg). A baseline electroretinogram (ERG) was recorded from each animal before any procedures were done and then weekly thereafter for the following 9 weeks.[44] The ERG protocol was always the same as described in the following text. Animals with traumatic crystalline lens damage, vitreous hemorrhage, or retinal detachment were excluded from analysis.

All intraocular injections were done in the right eye in the inferior temporal quadrant. After the baseline ERG was completed, the right eye was prepped with topical povidone iodine (10%). The procedure was done under a slit lamp using a microforceps to help stabilize the eye. After the limbus was clearly visualized, the conjunctiva and sclera were pierced with a 30-gauge needle. Then a total volume 5 μL of a 1 μM colloidal aqueous solution was injected into the vitreous cavity via pars plana using a microinjector (Hamilton, Reno, NV) and carefully avoiding the lens. After the procedure, topical instillation of analgesics (diclofenac 0.1%) and antibiotics (tobramicyn ointment 3.0 mg) were given as a single dose. Sham injections consisted of the same surgical procedure, except the eye was injected with sterile saline.

In the silicon-based and gold-based QD groups, four of eight eyes received only one dose of intravitreal QD. Two more received a second dose at week 3 of follow-up and the last two received a third dose at week 6 of follow-up. In the sham group, four of eight eyes received a single sham injection of saline at baseline. Of the remaining eyes, two received a second intravitreal sham injection and two more received a third sham injection at the same time points as in the QD groups. All injection procedures were done by the same investigator (JO). All animals were monitored every 4 to 5 minutes while under anesthesia by observing physical responses to a toe or skin pinch. The animals were monitored daily for the first 5 days, following injection for any signs of infection or alteration in behavior, and weekly thereafter.

ERGs were performed at baseline prior to any procedure and then weekly for 9 weeks. Before every measurement, the animals were anesthetized using the same protocol as in the intraocular injection. The cornea was additionally anesthetized using 1% tetracaine drops and coated with 1% methylcellulose. Using a handheld Ganzfeld stimulator, equipped with a commercial filter (Blue Kodak Wratten-Gelatin Filter; Kodak, Rochester, NY) to block wavelengths below 500 nm, bilateral ERGs were recorded simultaneously with electrodes (DTL Plus; Diagnosys, Lowell, MA) in contact with the ocular surface through a coating of 1% methylcellulose.[44] Monopolar needle electrodes (Advena, Hereford, UK) were placed in the cheek (reference) and the tail (ground). The animals were exposed to increasing intensities of light as follows: Step 1: Dark-adapted 0.01 ERG, with a 0.01 cd·s·m^{-2} stimulus and intervals of at least 2 s between flashes. Step 2: Dark-adapted 3.0 ERG, with a white 3.0 cd·s·m^{-2} stimulus and intervals of at least 10 s between stimuli. Step 3: Dark-adapted 3.0 oscillatory potentials, with a 3.0 cd·s·m^{-2} flash stimulus. Step 4: Light-adapted 3.0 ERG, with a 3.0 cd·s·m^{-2} stimulus and at least 0.5 s between flashes. Step 5: Light-adapted Flicker, with a flash rate of 30 Hz and intensity of 3.0 cd·s·m^{-2}. All animals went into a dark adaptation phase of at least 20 minutes before steps 1 to 3 and a light adaptation phase of at least 10 minutes before steps 4 and 5. A white background illumination was set at 30 cd·s·m^{-2} for steps 4 and 5. The electroretinography system (LKC Epic 4000; LKC Technologies, Gaithersburg, MD) was used for data filtering, acquisition, and averaging. A complete set of photopic, scotopic, and flicker responses were recorded each time. Every measurement was recorded a minimum of five times. All manual measurements were done by the same investigator (RVM) masked to the treatment groups.[44]

After 9 weeks all RCS rats in all groups were euthanized using carbon dioxide inhalation and cervical dislocation as a secondary method. All eyes were enucleated and placed in 2% paraformaldehyde/2.5% glutaraldehyde until processing. Using a razor blade, the anterior chamber and lens were removed 1 mm posterior to the limbus. The posterior poles of the eyes were preserved in paraffin. A diamond blade was used to cut sections 0.5 μm thick on an ultramicrotome. The
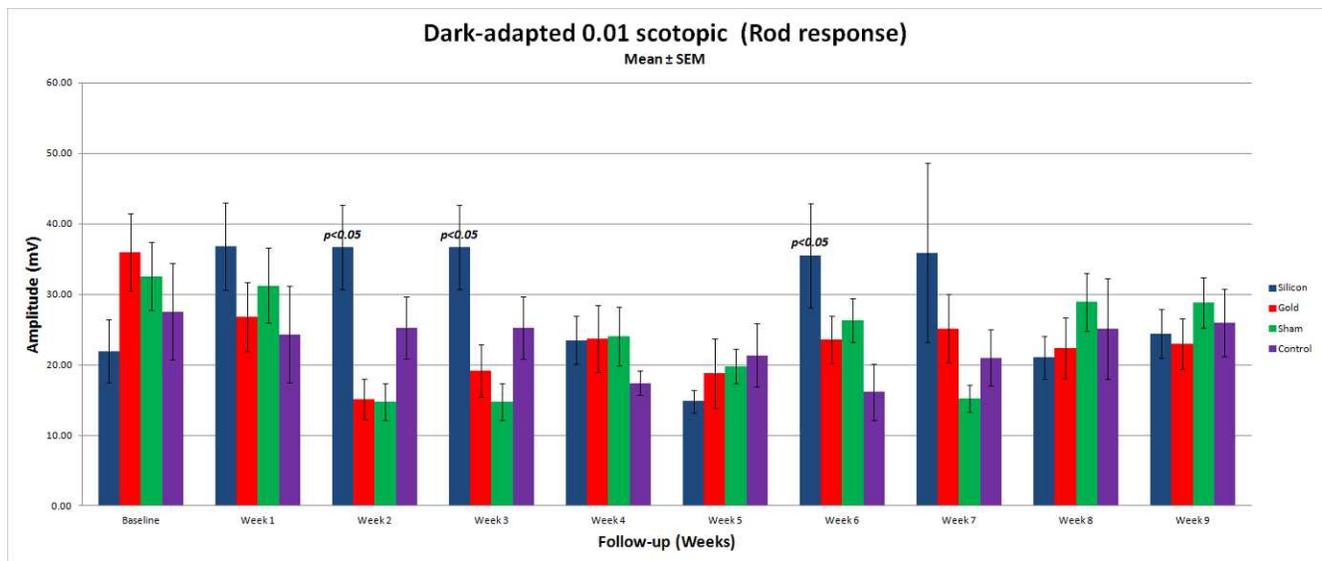
FIGURE 1. Mean and SEM of the rod response phase (step 1). The active group (silicon-based QDs) shows a statistically significant recovery of the amplitude at weeks 2, 3, and 6 of the follow-up.

sections were deparaffinized, rehydrated, and stained with hematoxylin and eosin for retina histologic analysis.

The slides were viewed through an automated microscope (Leica DM750; Leica Microsystems Inc., Buffalo Grove, IL) manipulated by a controller (J2-2000; Clemex Technologies Inc., Guimond Longueuil, Quebec, Canada) and with a ×20/0.70 objective. Digital images were captured by a high-performance digital camera (Qicam Fast 1394; QImaging, Surrey, BC, Canada), mounted on the top of the microscope. A total of three slides per each animal eye (≈96 slides) of the posterior pole were analyzed. Three images per slide (two from the periphery and one from the area centralis, ≈288 images) were stored as JPEG files and analyzed with a computer-assisted image program (Image-Pro plus 5.1; Media Cybernetics, Silver Spring, MD).[45–47] An area of interest was cropped manually in each image, to analyze separately the nuclei of the outer nuclear layer (ONL), the nuclei of the inner nuclear layer (INL), and the nuclei of the ganglion cell layer (GCL). The images were equalized and an automatic object count was done using the following color saturations: red (120–130), green (45–75), and blue (120–130). Then a watershed split and a cluster analysis were made for a more accurate count. The number of cell nuclei in the ganglion cell layer, inner nuclear layer, and outer nuclear layer was quantified by an observer masked to the treatment groups (RVM).[45–47]

Statistical analyses were made using a commercial spreadsheet (Excel 2007; Microsoft Corp., Redmond, WA). A one-way ANOVA test was used to identify differences in the variability of the means among groups, using a *P* value of less than 0.05 for statistical significance. Fisher's unprotected least significant difference test was used to assess statistical difference between means within study groups.

RESULTS

Retina Function by Groups

1. *Dark-adapted 0.01 scotopic (rod response):* This phase of the ERG elicits predominantly rod photoreceptor response. As expected in the RCS model, the wave amplitudes of the ERG waves declined in both control and sham groups. Although the sham and gold-based QD groups seemed to present a slight recovery of the function at weeks 4, 6, and 7 of follow-up, the changes failed to reach statistical significance. Conversely, the group injected with silicon-based QD showed a steady initial increase of the b-wave amplitude of the ERG

waves, reaching statistical significance at week 2 ($P < 0.001$) and week 3 ($P < 0.01$) postoperatively (weeks 6 and 7 of life). After week 3 postoperatively, the rod response decreased almost to the same level as that in the sham and control groups. Nevertheless, the group showed a recovery of the function after week 6 postoperatively (week 10 of life) ($P < 0.05$), which was maintained through week 7 but without reaching statistical difference at this point (Fig. 1).

2. *Dark-adapted 3.0 scotopic (combined rod–cone response):* This phase of the ERG elicits both rod and cone photoreceptor response. Although some a-waves were observed on some measurements, its presence was inconstant, which is a normal response in rodent ERG. The b-wave amplitude was measured for all light intensities presented. The amplitude of the b-wave was determined by measuring the difference from the trough of the electronegative a-wave (if present) or from the baseline to the peak of the electropositive b-wave. The b-wave amplitude in all groups decreased through the follow-up as expected in the RCS model. The amplitudes in the control and in the gold-based QD decreased at a slower pace, being significantly different with the sham and silicon-based QD group at week 1 ($P < 0.01$). There were no significant differences between the sham and gold-based QD groups at the same time point and the trend was not maintained during the rest of the follow-up.

3. *Dark-adapted 3.0 oscillatory potentials:* In this phase of the ERG, the amplitude of the oscillatory potential was measured using the automatic placement of the references by the software of the electroretinography system. The waves showed a progressive decrease in their amplitude in all groups through the study. Although both QD groups and control decreased their amplitude at a slower pace than that of the sham group, there were no statistically significant differences among them. Nevertheless, the silicon-based QD showed a slight recovery of the function at week 5 of follow-up (week 9 of life) with statistical significance ($P < 0.05$).

4. *Light-adapted 3.0 ERG (single-flash cone response):* Overall, the amplitudes tended to decrease in all groups. The active group with the silicon-based QD showed an
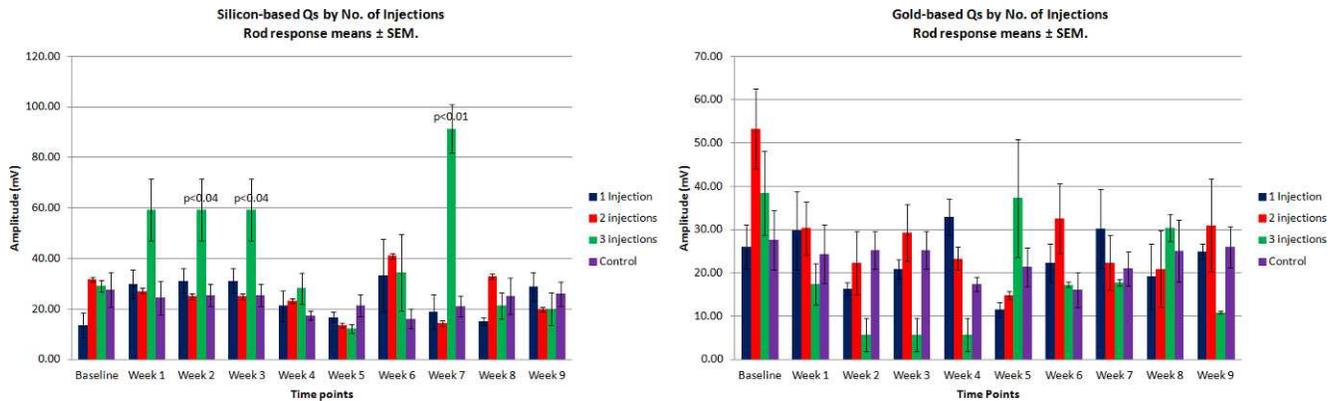
FIGURE 2. Comparative chart of the active and inactive groups (silicon-based versus gold-based QDs) rode response (step 1) by the number of injections (means and SEM). The three-injection subgroups in the silicon-based QD group (*right*) showed a significant recovery of the amplitude after the first injection (weeks 2 and 3) and again after the third (week 7). In the gold-based QD group (*left*), the three-injection subgroup showed a mild recovery at weeks 5 and 8, probably due to the injection procedure.

increase in the amplitude during weeks 2 and 3 of follow-up but without reaching statistical significance. A similar spike was observed in both QD groups during week 7 of follow-up but without statistical significance.

5. *Light-adapted 3.0 flicker ERG (30-Hz flicker):* The photopic 30-Hz flicker is a measurement of cone function. It has two recordable phases: the amplitude and implicit time. The wave's amplitude initially decreased in all groups. The silicon-based QD group showed a slight recovery of the amplitude at week 4 of follow-up, being significant against the sham and control ($P < 0.01$) but not against the gold-based QD group ($P = 0.1$). After week 6 of follow-up, all groups showed a significant recovery of the wave's amplitude but the effect was lost by the end of the study. Regarding the implicit time, all subgroups showed an increase in the implicit time through all the weeks of the follow-up but without a significant difference among them or against the control group.

Retina Function by Number of Injections

1. *Dark-adapted 0.01 scotopic (rod response):* In the silicon-based QD group, all subgroups showed a slight increase in the amplitude from week 1 to week 3 of follow-up but not different from that in the control group. It is noteworthy to mention that in the subgroup scheduled to receive three injections, the initial dose produced a steady increase in the wave's amplitude for 3 weeks, reaching statistical significance at weeks 2 ($P < 0.05$) and 3 ($P < 0.05$) of follow-up. This effect was lost immediately but recovered strongly at week 7 after the third injection at week 6 of follow-up ($P < 0.01$). In the gold-based subgroups, the amplitude decreased in an irregular pattern. However, in the subgroup scheduled to received three injections, despite showing a more marked decrease of the amplitude during the first weeks of follow-up, the amplitude recovered at week 5 (2 weeks after the second injection, $P < 0.05$). A similar response was seen at the 8th week of follow-up, 2 weeks after the third injection but without reaching statistical difference (Fig. 2).

2. *Dark-adapted 3.0 scotopic (combined rod–cone response):* All the silicon-based QD subgroups showed a progressive loss of the b-wave amplitude through the follow-up. The amplitude in the gold-based subgroups decreased as well. Nevertheless, all three subgroups

showed slight recovery of the b-wave amplitude from weeks 6 to 7 of follow-up, but without reaching statistical significance.

3. *Dark-adapted 3.0 oscillatory potentials:* All of the subgroups in the silicon-based QD group showed a sustained decrease of the amplitude. However, all of them also showed a small peak of recovery at week 5 of follow-up, being statistically significant in the subgroup scheduled to receive three injections ($P < 0.05$). The subgroups in the gold-based QD group behaved in a similar manner. There was a peak of recovery in the two-injection group at weeks 7 and 8 of follow-up, which reached statistical significance ($P < 0.05$).

4. *Light-adapted 3.0 ERG (single-flash cone response):* Overall, all the subgroups in the silicon-based QD group decreased the amplitude of the b-wave. Although there were two mild peaks of recovery at weeks 3 and 7 of follow-up, especially in the subgroup with only one injection, they failed to reach statistical significance among them and against the control.

5. *Light-adapted 3.0 flicker ERG (30-Hz flicker):* Both active groups showed a progressive decrease in the flicker amplitude. The silicon-based subgroups showed a recovery peak at week 7 of follow-up, especially in the three-injections subgroup, which was significantly different from that of the other two subgroups ($P < 0.01$) but not against the control. Something similar happened in the two-injections subgroup of the gold-based QD group at week 7 of follow-up in which the increase of the amplitude reached statistical significance against the other two subgroups ($P < 0.01$) but not against the control and slowly decreasing during the final 2 weeks of follow-up. Regarding the implicit time, all subgroups showed an increase in the implicit time through all the weeks of the follow-up but without a significant difference among them or against the control group.

Retina Histology

A total of 72 slides and 216 images were analyzed. The overall cell count in all three nuclear layers of the retina is summarized in the Table. There were no instances of traumatic cataract, vitreous hemorrhage, or retinal detachment in any of the eyes (Fig. 3). During the pathology procedures and slides' manufacturing, the retina architecture from the sham group was severely damaged, preventing visual differentiation be-

TABLE. Total Nuclei Counts by the Different Layers of the Retina in the QD Groups and in the Control Group

Retina Layer	Silicon	Gold	Control
Outer nuclear layer	334.4 ± 165.99	156.36 ± 75.21	121.61 ± 20.78
Inner nuclear layer	564.79 ± 134.53	667.49 ± 300.42	481 ± 108.66
Ganglion cell layer	65.94 ± 19.79	65.65 ± 26.87	43.19 ± 11.52

tween the different cell layers. Therefore, no cell counts were made from any of these slides.

Outer Nuclear Layer. At the end of the follow-up (week 14 of life) in the RCS model, we should expect a very thin retina with cellular debris, the hallmark of the retinal degeneration model. In the control group, ONL thickness decreased until it was merely one or two cells thick (Fig. 3C). A similar decrease in the cell nuclei count was observed in the gold-based QD group. Conversely, in the silicon-based QD group, ONL thickness seems to have been preserved during the entire follow-up, which cell nuclei count reached statistical significance against the gold-based QD and control groups ($P < 0.01$, Fig. 3A).

Inner Nuclear Layer. This layer was better preserved in all three groups. However, the eyes that received the QDs showed a trend of having higher nuclei count than that of the control group. There were no statistical differences among the QD groups (Figs. 3A, 3B).

Ganglion Cell Layer. Both QD groups had a better preserved GCL than the control group. Although both QD groups had a statistically significant difference with the control group ($P < 0.01$), there were no statistical differences when comparing both QD groups ($P = 0.9$).

DISCUSSION

Direct electrical stimulation of the nervous system has proved to be a promising therapy in several neurodegenerative diseases by exerting a neuroprotective effect over healthy cells through the activation of the production of survival and growth factors.[29,30] Although its benefits have been documented in several studies, we have barely begun to understand its mechanism of action and possible applications. Previous efforts to apply the benefits of ES to the retina have been made and various routes of energy delivery have been proposed, including: noninvasive, transcorneal contact sys-
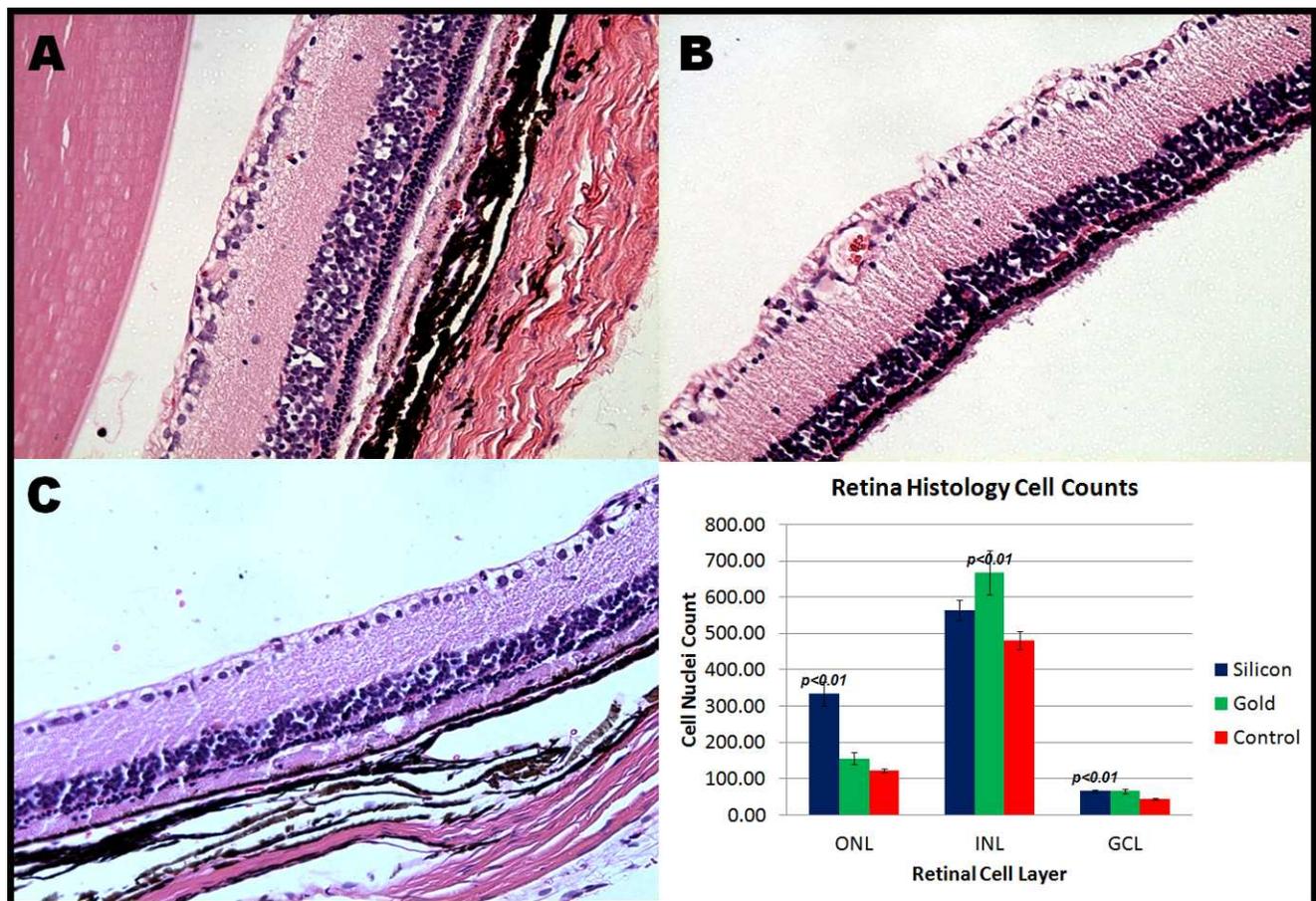

FIGURE 3. Histologic examination by groups. (**A**) Silicon-based QD group: this image shows well-preserved nuclei in all retinal layers. It is important to note that the ONL is remarkably well preserved despite the age of the rat. (**B**) Gold-based QD group: the nuclei are well preserved also but the ONL is thinner than the one observed in 3A. (**C**) Control group: there is a marked decrease in the thickness of the layers. In the *lower right corner* there is a graphical representation of the total nuclei counts by the different layers of the retina.

tems, and intraocular and suprachoroidal-transretina implants.[48-52] The duration of ES has ranged from very brief periods, to long-term studies (5 years or longer). Despite the route of delivery or duration of the stimuli, many studies demonstrate that there is a definite beneficial effect in animal models and in human trials as well.[48] In the present study, we have explored the possibility of using nanoparticles made from semiconductor crystals (quantum dots) as a way to electrically stimulate retinal cells at a molecular level, to elicit a change in the electrical pattern and survival rate of retina cells in an established model of retinal degeneration. Our results are consistent with previous reports in which ES has been shown to prevent cell death in all three retinal nuclear layers by demonstrating a higher nuclei count. Our study has also shown a change in the retinal electrical activity. Although the changes were transient, there is a recurrent effect that cannot be attributed solely to the injection procedure.

Retinal degeneration and its subsequent irreversible vision loss is a feared disability that is currently the focus of several investigations.[9] Some of them are aimed to prevent retina degeneration before it happens, like gene therapy and ES research.[9] The former uses a mechanical or biological vector (viruses) to deliver a specific gene and promoter sequence, to activate or supplant a deficiency in the DNA coding.[53] Others like stem cell and retina transplant research are aimed to repopulate a definite cell line (photoreceptors, RPE), to regain function or to replace a complete degenerated retina with a full thickness transplant from a donor.[53] Finally, the complete substitution of the retinal function with prosthesis, to achieve a useful vision, is the goal of several artificial vision projects around the world.[48,54]

The first successful attempt of gene augmentation through a viral vector was completed on June 2009 at the Children's Hospital of Philadelphia.[55,56] In this study 12 patients with Leber congenital amaurosis (ages ranged from 8 to 44 years) were injected once unilaterally into the subretinal space with a recombinant adeno-associated virus vector carrying the human RPE65 cDNA, in volumes ranging from 0.15 to 1.0 mL. The results prove that the therapy was feasible and safe after 2.5 years of follow-up. Moreover, all patients showed at least a 2 log-unit increase in pupillary light response and age-dependent visual recovery, with the children deriving the most benefit.[55,56] The five children recruited in this study gained ambulatory vision and are able to participate in normal classroom and athletic endeavors.[55,56] More studies are under way, addressing a variety of diseases including retinitis pigmentosa.[57,58]

Stem-cell therapy is a potentially therapeutic approach that uses the pluripotent and self-renewing properties of the stem cells, to increase cell survival through the induction of the production of growth factors by genetically manipulating stem cells, including ciliary neurotrophic factor, fibroblast growth factor 2, brain-derived neurotrophic factor, and glial-derived neurotrophic factor, although there may be other factors yet to be discovered.[53,59] This approach has been used most successfully in animal models of photoreceptor or retina ganglion cells rescue following transplant into the vitreous cavity, subretinal space, or optic nerve.[9] In addition, cell line replacements are being investigated by differentiating specific cell lines (photoreceptor, RPE cells, and retinal ganglion cells) from different kinds of stem cells like bone marrow stem cells, retinal stem cells, and reprogrammed fibroblasts. Although migration and integration into the retina and expression of photoreceptor-specific surface markers have been observed, synapse formation and functional recovery have been exceptionally rare.[9,60] The fact that RPE cells do not have any synaptic connection makes them more suitable candidates for replacement by stem cell manipulation than photoreceptors or inner retina cells.[53,61] In January of 2012, a team of researchers from UCLA reported the first successful transplant of human embryonic stem cells in two patients (one with the dry form of age-related macular degeneration and another with Stargardt disease). The transplanted cells showed no signs of hyper-proliferation, tumorigenicity ectopic tissue formation, or apparent rejection and neither patient lost vision.[61]

The complete substitution of retinal function with an artificial prosthesis has been an area of intense interest.[53] The first retinal prosthesis for the blind was proposed by Tassiker et al.,[54] and consisted of a light-sensitive selenium photodiode cell placed behind the retina. To date, at least 23 different groups are conducting extensive research in the field around the world. There are several types of prospective retinal prostheses, their physical properties ranging from purely electromechanical devices to biochemical and complex biomechanical devices.[48,54,62] Currently they have been divided according to the anatomic location where they are placed. There are suprachoroidal prostheses, subretinal prostheses, epiretinal prostheses, direct optic nerve stimulation, and cortical prostheses. Their mechanism of action is based on the principle that electric stimulation of the human eye can activate the retina and elicit an artificial sensation of light termed electrophosphene.[54] This is achieved because the light absorbed by the electrodes in the prostheses can depolarize and form action potentials in ganglion cells, ganglion cells axons, or directly depolarize cells in the retinal network such as bipolar or amacrine cells (which propagate the visual signal to the ganglion cells) or neurons in the visual cortex.[48,54] A similar process occurs in the digital camera–based retinal prostheses in which the image is first processed and converted to electrical currents to stimulate the remaining retinal cells or visual cortex of the brain.[48,54]

Each of them has several advantages and disadvantages. In the epiretinal approach, the stimulation electrode array is placed in the vitreous cavity directly over the retina surface. Although it is a less invasive design that does not occlude the retina vasculature and can be monitored ophthalmoscopically, it prevents the light from reaching the retina; therefore, it must replicate the complicated phenomenon of phototransduction, requiring more complex designs.[54] The Argus II prototype is the leading device of its kind developed by Humayun et al.[63] at Doheny Eye Institute, which consists of a 60 electrode array with a very sophisticated neural interface and uses wireless technology to transmit power and data. The prototype is currently being evaluated in a 3-year, multicenter phase-2 clinical trial and is the result of collaboration between the Department of Energy, six National Laboratories, and three universities (ClinicalTrials.gov numbers NCT00407602, NCT01490827).

In the subretinal approach, the prostheses make use of the intrinsic retinal pathway, which may produce a more natural excitation of the ganglion cells.[54,62] They have a major limitation in that they stand between the outer retina and its natural supply of oxygen: the choriocapillaris.[54] Long-term studies have demonstrated pronounced photoreceptor degeneration in the area of the implant.[64] Another drawback is the limited space and the local heat generation by the power source.[54,64] The Okayama University–type retinal prosthesis is a novel type of retinal prosthesis, which uses photoelectric dye molecules that absorb light to generate electric potentials.[48] This approach more closely mimics the way that normal photoreceptors convert light into electric signals. The photoelectric dye is distributed on a polyethylene film and placed in the subretinal space. In a recent study, Matsuo et al.[48] proved the safety and efficacy of the prototype in an RCS rat model by demonstrating intracellular calcium elevation as a signal of cellular activity of depolarized neurons and glial cells.

In the suprachoroidal approach, the stimulating electrode lies inside or on the surface of the sclera. Their advantages are that they pose little risk for retinal detachment, do not prevent oxygen flow from the choriocapillaris to the retina, and are adjacent to the outer retina.[54] Nevertheless, due to the fact that they are located behind the RPE, which has a higher resistance to electric current flow (5- to 15-fold higher than the retina), they require higher power than the regular subretinal or epiretinal devices.[54]

Regardless of the type of retinal prosthesis, a common drawback for all of them is the fact that they require an operating room–based surgery, which carries with it the risk of surgical complications such as retinal detachment, vitreous hemorrhages, and infection.

Nanotechnology makes it possible to deliver electrical stimulation at a cellular (even molecular) level. This is a relatively new science that studies new ways to manipulate matter on an atomic and molecular-level scale (particles from 1 to 100 nm in size).[32,53] Even though in ophthalmology the efforts have been aimed mainly to develop new drug delivery systems, their potential applications are wide ranging.

There are several considerations in determining the effects of intraocular photoactive QD in this study: First the positive results might be due to two factors: (1) The mechanical trauma to the eye is a well-known stimulus for the production of growth factors that may confound the results by attenuating the progressive retinal deterioration. In our study we try to ameliorate this factor by including a sham and a naïve control group. The mild recovery of electrical function in the gold-based (inactive) QD group is proof of this phenomenon. (2) The electrical stimulation of the retina by using silicon-based QD seems to have a brief, but significant effect on rat ERGs, and mainly on the rod's response.

Second, there are factors that may have decreased the efficacy of the silicon-based QD used in the study. Notably, we used one kind of active QD in a fixed concentration. Even though there was a definite effect on the ERG, there might be still room to improve the results by increasing the particle concentration. Second, silicon was selected because of the track record of biocompatibility. Other materials, such as cadmium/selenium quantum dots, may have a more pronounced effect. However, despite that studies with x-ray photoelectron spectroscopy have shown a surface potential shift up to −0.13 eV when stimulated with white light, the magnitude and extent of the effect of the electrical field of a single particle or group of particles may have, has not been fully studied yet and may have an impact in selecting the appropriate QD dose and material.[65] (3) Although our group did not conduct any surface characterization of the nanoparticles provided by the manufacturer, the thermodynamic controlled colloidal precipitation technique used for its synthesis may end in the production of either hydrogen-terminated or halogen-terminated nanoparticles and hence highly prone to oxidation.[66] The addition of sodium dodecyl-benzenesulfonate surfactant coating serves as a method of molecule passivation and adds a hydrophilic interface for stability in aqueous media.[67] Nevertheless, small changes in the pH after injection may remove the coating, leaving the nanoparticles prone to form bonds to carbon or oxygen, which may in turn have an effect in the observed results of this study.[68] (4) The formation of aggregates of nanoparticles during the injection procedure is also a possibility; however, characterization of the nanoparticles by other groups with transmission electron microscopy and energy dispersive spectrometry have shown stable monodisperse diameters of the silicon nanoparticles.[68]

In summary, the use of silicon-based quantum dots in the RCS rat model seems to be safe, with no evident toxic reactions and to have a beneficial effect by prolonging the cell survival rate in an established model of retinal degeneration. The procedure is potentially safer than other methods of retina eclectic stimulation (retinal prosthesis) that require surgery, whereas the former only needs an intravitreal injection (can be performed in an office setting and also be repeatable). The particles induced a definite but transient change in the waves of the ERG by increasing the amplitude of the b-wave, especially in the rod's response. Finally, the ability to stimulate the retina at a cellular level and to promote local production of growth factors would allow us to address potentially blinding disease at a stage prior to visual loss and prevent or delay progression.

References

1. Salomao SR, Mitsuhiro MR, Belfort R Jr. Visual impairment and blindness: an overview of prevalence and causes in Brazil. *An Acad Bras Cienc*. 2009;81:539–549.

2. Congdon NG, Friedman DS, Lietman T. Important causes of visual impairment in the world today. *JAMA*. 2003;290:2057–2060.

3. Schellini SA, Durkin SR, Hoyama E, et al. Prevalence and causes of visual impairment in a Brazilian population: the Botucatu Eye Study. *BMC Ophthalmol*. 2009;9:8.

4. Resnikoff S, Pascolini D, Etya'ale D, et al. Global data on visual impairment in the year 2002. *Bull World Health Organ*. 2004;82:844–851.

5. West S, Sommer A. Prevention of blindness and priorities for the future. *Bull World Health Organ*. 2001;79:244–248.

6. Patel DK, Tajunisah I, Gilbert C, Subrayan V. Childhood blindness and severe visual impairment in Malaysia: a nationwide study. *Eye*. 2011;25:436–442.

7. Gilbert C, Foster A, Negrel AD, Thylefors B. Childhood blindness: a new form for recording causes of visual loss in children. *Bull World Health Organ*. 1993;71:485–489.

8. den Hollander AI, Black A, Bennett J, Cremers FP. Lighting a candle in the dark: advances in genetics and gene therapy of recessive retinal dystrophies. *J Clin Invest*. 2010;120:3042–3053.

9. Dahlmann-Noor A, Vijay S, Jayaram H, Limb A, Khaw PT. Current approaches and future prospects for stem cell rescue and regeneration of the retina and optic nerve. *Can J Ophthalmol*. 2010;45:333–341.

10. Bunce C, Wormald R. Leading causes of certification for blindness and partial sight in England & Wales. *BMC Public Health*. 2006;6:58.

11. McGwin G, Khoury R, Cross J, Owsley C. Vision impairment and eye care utilization among Americans 50 and older. *Curr Eye Res*. 2010;35:451–458.

12. Brown G, Brown MM. Let us wake the nation on the treatment for age-related macular degeneration. *Curr Opin Ophthalmol*. 2010;21:169–171.

13. Rein DB, Wittenborn JS, Zhang X, Honeycutt AA, Lesesne SB, Saaddine J. Forecasting age-related macular degeneration through the year 2050: the potential impact of new treatments. *Arch Ophthalmol*. 2009;127:533–540.

14. Apte RS, Scheufele TA, Blomquist PH. Etiology of blindness in an urban community hospital setting. *Ophthalmology*. 2001;108:693–696.

15. Smith AF, Smith JG. The economic burden of global blindness: a price too high! *Br J Ophthalmol*. 1996;80:276–277.

16. Chakravarthy U, Evans J, Rosenfeld PJ. Age related macular degeneration. *BMJ*. 2010;340:c981.

17. Maier PC, Funk J, Schwarzer G, Antes G, Falck-Ytter YT. Treatment of ocular hypertension and open angle glaucoma: meta-analysis of randomised controlled trials. *BMJ*. 2005;331:134.

18. Weise J, Isenmann S, Klocker N, et al. Adenovirus-mediated expression of ciliary neurotrophic factor (CNTF) rescues axotomized rat retinal ganglion cells but does not support axonal regeneration in vivo. *Neurobiol Dis*. 2000;7:212–223.

19. Wang N, Zeng M, Ruan Y, et al. Protection of retinal ganglion cells against glaucomatous neuropathy by neurotrophin-producing, genetically modified neural progenitor cells in a rat model. *Chin Med J (Engl)*. 2002;115:1394–1400.

20. Pease ME, Zack DJ, Berlinicke C, et al. Effect of CNTF on retinal ganglion cell survival in experimental glaucoma. *Invest Ophthalmol Vis Sci*. 2009;50:2194–2200.

21. Bajd T, Gregoric M, Vodovnik L, Benko H. Electrical stimulation in treating spasticity resulting from spinal cord injury. *Arch Phys Med Rehabil*. 1985;66:515–517.

22. Capus L, Melatini A, Zorzon M, et al. Chronic bilateral electrical stimulation of the subthalamic nucleus for the treatment of advanced Parkinson's disease. *Neurol Sci*. 2001; 22:57–58.

23. Tesfaye S, Watt J, Benbow SJ, Pang KA, Miles J, MacFarlane IA. Electrical spinal-cord stimulation for painful diabetic peripheral neuropathy. *Lancet*. 1996;348:1698–1701.

24. Chung BPH, Cheng BKK. Immediate effect of transcutaneous electrical nerve stimulation on spasticity in patients with spinal cord injury. *Clin Rehabil*. 2010;24:202–210.

25. Laszig R, Aschendorff A. Cochlear implants and electrical brainstem stimulation in sensorineural hearing loss. *Curr Opin Neurol*. 1999;12:41–44.

26. Watanabe M, Fukuda Y. Survival and axonal regeneration of retinal ganglion cells in adult cats. *Prog Retin Eye Res*. 2002; 21:529–553.

27. Schmid H, Herrmann T, Kohler K, Stett A. Neuroprotective effect of transretinal electrical stimulation on neurons in the inner nuclear layer of the degenerated retina. *Brain Res Bull*. 2009;79:15–25.

28. Pardue MT, Phillips MJ, Yin H, et al. Neuroprotective effect of subretinal implants in the RCS rat. *Invest Ophthalmol Vis Sci*. 2005;46:674–682.

29. Saygili E, Schauerte P, Kuppers F, et al. Electrical stimulation of sympathetic neurons induces autocrine/paracrine effects of NGF mediated by TrkA. *J Mol Cell Cardiol*. 2010;49:79–87.

30. Baba T, Kameda M, Yasuhara T, et al. Electrical stimulation of the cerebral cortex exerts antiapoptotic, angiogenic, and anti-inflammatory effects in ischemic stroke rats through phosphoinositide 3-kinase/Akt signaling pathway. *Stroke*. 2009;40: e598–e605.

31. Rosenthal SJ, Chang JC, Kovtun O, McBride JR, Tomlinson ID. Biocompatible quantum dots for biological applications. *Chem Biol*. 2011;18:10–24.

32. Barroso MM. Quantum dots in cell biology. *J Histochem Cytochem*. 2011;59:237–251.

33. Yang H. Nanoparticle-mediated brain-specific drug delivery, imaging, and diagnosis. *Pharm Res*. 2010;27:1759–1771.

34. Pappas TC, Wickramanyake WM, Jan E, Motamedi M, Brodwick M, Kotov NA. Nanoscale engineering of a cellular interface with semiconductor nanoparticle films for photo-electric stimulation of neurons. *Nano Lett*. 2007;7:513–519.

35. Leschkies KS, Divakar R, Basu J, et al. Photosensitization of ZnO nanowires with CdSe quantum dots for photovoltaic devices. *Nano Lett*. 2007;7:1793–1798.

36. Brigger I, Chaminade P, Desmaele D, et al. Near infrared with principal component analysis as a novel analytical approach for nanoparticle technology. *Pharm Res*. 2000;17:1124–1132.

37. Yamamoto S, Manabe N, Fujioka K, Hoshino A, Yamamoto K. Visualizing vitreous using quantum dots as imaging agents. *IEEE Trans Nanobiosci*. 2007;6:94–98.

38. Wang HC, Brown J, Alayon H, Stuck BE. Transplantation of quantum dot-labelled bone marrow-derived stem cells into the vitreous of mice with laser-induced retinal injury: survival, integration and differentiation. *Vision Res*. 2010;50:665–673.

39. Hardman R. A toxicologic review of quantum dots: toxicity depends on physicochemical and environmental factors. *Environ Health Perspect*. 2006;114:165–172.

40. Pardue MT, Phillips MJ, Yin H, et al. Possible sources of neuroprotection following subretinal silicon chip implantation in RCS rats. *J Neural Eng*. 2005;2:S39–S47.

41. Mullen RJ, LaVail MM. Inherited retinal dystrophy: primary defect in pigment epithelium determined with experimental rat chimeras. *Science*. 1976;192:799–801.

42. Gal A, Li Y, Thompson DA, et al. Mutations in MERTK, the human orthologue of the RCS rat retinal dystrophy gene, cause retinitis pigmentosa. *Nat Genet*. 2000;26:270–271.

43. Bok D, Hall MO. The role of the pigment epithelium in the etiology of inherited retinal dystrophy in the rat. *J Cell Biol*. 1971;49:664–682.

44. Rosolen SG, Kolomiets B, Varela O, Picaud S. Retinal electrophysiology for toxicology studies: applications and limits of ERG in animals and ex vivo recordings. *Exp Toxicol Pathol*. 2008;60:17–32.

45. Saad HA, Terry MA, Shamie N, et al. An easy and inexpensive method for quantitative analysis of endothelial damage by using vital dye staining and Adobe Photoshop software. *Cornea*. 2008;27:818–824.

46. Francisco JS, Moraes HP, Dias EP. Evaluation of the Image-Pro Plus 4.5 software for automatic counting of labeled nuclei by PCNA immunohistochemistry. *Braz Oral Res*. 2004;18:100–104.

47. Olson JL, Velez-Montoya R, Erlanger M. Ocular biocompatibility of nitinol intraocular clips. *Invest Ophthalmol Vis Sci*. 2012;53:354–360.

48. Matsuo T, Uchida T, Takarabe K. Safety, efficacy, and quality control of a photoelectric dye-based retinal prosthesis (Okayama University-type retinal prosthesis) as a medical device. *J Artif Organs*. 2009;12: 213–225.

49. Humayun MS, de Juan E Jr, Dagnelie G, Greenberg RJ, Propst RH, Phillips DH. Visual perception elicited by electrical stimulation of retina in blind humans. *Arch Ophthalmol*. 1996;114:40–46.

50. de Balthasar C, Patel S, Roy A, et al. Factors affecting perceptual thresholds in epiretinal prostheses. *Invest Ophthalmol Vis Sci*. 2008;49:2303–2314.

51. Besch D, Sachs H, Szurman P, et al. Extraocular surgery for implantation of an active subretinal visual prosthesis with external connections: feasibility and outcome in seven patients. *Br J Ophthalmol*. 2008;92:1361–1368.

52. Fujikado T, Morimoto T, Kanda H, et al. Evaluation of phosphenes elicited by extraocular stimulation in normals and by suprachoroidal-transretinal stimulation in patients with retinitis pigmentosa. *Graefes Arch Clin Exp Ophthalmol*. 2007;245:1411–1419.

53. Chiang A, Haller JA. Vitreoretinal disease in the coming decade. *Curr Opin Ophthalmol*. 2010;21:197–202.

54. Cohen ED. Prosthetic interfaces with the visual system: biological issues. *J Neural Eng*. 2007;4:R14–31.

55. Maguire AM, High KA, Auricchio A, et al. Age-dependent effects of RPE65 gene therapy for Leber's congenital amaurosis: a phase 1 dose-escalation trial. *Lancet*. 2009;374:1597–1605.

56. Simonelli F, Maguire AM, Testa F, et al. Gene therapy for Leber's congenital amaurosis is safe and effective through 1.5 years after vector administration. *Mol Ther*. 2010;18:643–650.

57. Cideciyan AV, Aleman TS, Boye SL, et al. Human gene therapy for RPE65 isomerase deficiency activates the retinoid cycle of vision but with slow rod kinetics. *Proc Natl Acad Sci USA*. 2008;105:15112–15117.

58. Bainbridge JW, Smith AJ, Barker SS, et al. Effect of gene therapy on visual function in Leber's congenital amaurosis. *N Engl J Med*. 2008;358:2231–2239.

59. Baker PS, Brown GC. Stem-cell therapy in retinal disease. *Curr Opin Ophthalmol*. 2009;20:175–181.

60. MacLaren RE, Pearson RA, MacNeil A, et al. Retinal repair by transplantation of photoreceptor precursors. *Nature*. 2006; 444:203–207.

61. Schwartz SD, Hubschman JP, Heilwell G, et al. Embryonic stem cell trials for macular degeneration: a preliminary report. *Lancet*. 2012;379:713–720.

62. Chow AY, Bittner AK, Pardue MT. The artificial silicon retina in retinitis pigmentosa patients (an American Ophthalmological Association thesis). *Trans Am Ophthalmol Soc*. 2010;108: 120–154.

63. Stieglitz T. Development of a micromachined epiretinal vision prosthesis. *J Neural Eng*. 2009;6:065005.

64. Pardue MT, Ball SL, Phillips MJ, et al. Status of the feline retina 5 years after subretinal implantation. *J Rehabil Res Dev*. 2006; 43:723–732.

65. Ekiz OO, Mizrak K, Dana A. Chemically specific dynamic characterization of photovoltaic and photoconductivity effects of surface nanostructures. *ACS Nano*. 2010;4:1851–1860.

66. Ruizendaal L, Pujari SP, Gevaerts V, Paulusse JM, Zuilhof H. Biofunctional silicon nanoparticles by means of thiol-ene click chemistry. *Chem Asian J*. 2011;6:2776–2786.

67. Eckhoff DA, Sutin JD, Clegg RM, Gratton E, Rogozhina EV, Braun PV. Optical characterization of ultrasmall Si nanoparticles prepared through electrochemical dispersion of bulk Si. *J Phys Chem B*. 2005;109:19786–19797.

68. Shiohara A, Hanada S, Prabakar S, et al. Chemical reactions on surface molecules attached to silicon quantum dots. *J Am Chem Soc*. 2010;132:248–253.